Microstructure and Electrochemical Behaviour of some SnO_2-based Inert Electrodes in Aluminium Electrolysis

Ana-Maria Popescu, Suzana Mihaiu, and Stefania Zuca
Romanian Academy, Institute of Physical Chemistry “I.G.Murgulescu”,
Splaiul Independentei 202, Bucharest 77208, Romania
Reprint requests to A.-M. P.; Fax: +4-01-3121147; E-mail: ampop@chimfiz.icf.ro

Z. Naturforsch. **57 a,** 71–75 (2002); received August 20, 2001

Presented at the NATO Advanced Study Institute, Kas, Turkey, May 4 - 14, 2001.

Some types of anodes that could replace the usual carbon anodes in aluminium production by the Hall-Heroult process are based on SnO_2. The present investigation deals with SnO_2-Sb_2O_3-CuO ceramics having an SnO_2 content of $\geq$96%), Sb_2O_3 and CuO being dopants. The ceramic pellets, thermally treated at 1400 °C for 4 hours, were analysed by X-ray diffraction and IR spectroscopy. The structural analysis of the samples evidenced an $SnO_{2\,(ss)}$ type solid solution. All samples were electronically conductive (small negative values of the Seebeck coefficients), having an activation energy ranging within 0.02 - 0.3 eV.

The anodic polarisation curves obtained with those anodes in an electrolyte of 88% Na_3AlF_6, 7% Al_2O_3 and 5% CaF_2 were studied. The results were correlated with the microstructure of the investigated samples.

Key words: SnO_2 Ceramics; Inert Anodes; Anode Polarisation; Molten Salts.

1. Introduction

Replacement of the consumable electroconductive carbon anodes of the Hall-Heroult cell by inert SnO_2-based anodes has interested many researchers for a long time [1 - 4]. Our studies in this field were centred on ceramics based on Sb_2O_3 and CuO doped SnO_2 [5, 6].

Dense electronconductive ceramics containing more than 90wt% SnO_2 were used. The optimum composition (from the viewpoint of the densification and electrical conductivities) was found to be 96wt% SnO_2, 2wt% Sb_2O_3, and 2wt% CuO. In the papers [7 - 9] the electrochemical behaviour of this anode material in a cryolite-alumina bath was studied, and the current efficiency (CE) was evaluated to be ∼92%, compared to 87% of carbon anodes.

The optimum working parameters of the electrolysis cell, i. e. temperature, current density, interelectrode distance and electrolyte composition were determined. Due to the fact that anode corrosion appears to be the main obstacle for the use of inert anodes in commercial cells [10], the corrosion rate of SnO_2-based inert anodes was studied as a function of the interelectrode distance (ACD), current density (CD) and concentration of Al_2O_3 and LiF [11].

During the electrochemical investigations some irregularities were found (it seemed that a small amount of oxygen was consumed on the anode).

To understand the causes of these phenomena to diminish or remove them, we studied the chemical processes between the three oxides (SnO_2, Sb_2O_3, CuO) taking place during the thermal treatment.

The studies performed in the SnO_2-Sb_2O_3-CuO ternary system underlined the complex phase relationship [12 - 14].

Thus, tin dioxide and antimony oxide give a limited solid solution with rutile type structure of the $Sn_{1-x}Sb_xO_2$ form. Copper (II) oxide does not react chemically with SnO_2, but it forms a eutectic melt that improves significantly the sintering.

When Sb_2O_3 and CuO coexist with SnO_2, the chemical reaction of CuO and Sb_2O_3 takes place preferentially, forming $CuSb_2O_6$ and/or $Cu_4SbO_{4.5}$ binary compounds.

In an O_2 atmosphere or at high pressure, for a molar ratio $CuO/Sb_2O_3 > 4$ the $Cu_9Sb_4O_{19}$ compound can also be formed [15]. Up to 25mol% $CuSb_2O_6$ with

Table 1. Starting composition, phase composition and ceramic properties of the samples thermally treated 4 hours at 1400 °C.

	Oxide composition (wt%)			CuO/Sb_2O_3	Phase composition			Ceramic properties		
Sample	SnO_2	Sb_2O_3	CuO	molar ratio	phase	$V(\mathrm{Å}^3)$	ΔV * %	$\Delta l/l$(%)	P_a(%)	d(g/cm^3)
S_1	98	2	–	–	$SnO_{2(ss)}$	71.4	–0.14	0	8.8	4.73
S_2	98	–	2	–	$SnO_{2(ss)}$	–	–	–12.6	0	6.48
S_3	97.5	2	0.5	0.91	$SnO_{2(ss)}$	71.4	–0.14	–4	7.16	5.01
S_4	98	1	1	3.71	$SnO_{2(ss)}$	71.2	–0.4	–18	0	6.85
S_5	96	2	2	3.70	$SnO_{2(ss)}$	71.2	–0.4	–11.3	0	6.55

* $\Delta V = \frac{V_{\mathrm{sample}} - V_{\mathrm{SnO_2}}}{V_{\mathrm{SnO_2}}} \cdot 100$ [%], $V_{\mathrm{SnO_2}} = 71.5\ \mathrm{Å}^3$.

trirutile type structure dissolves in the SnO_2 lattice. A solid solution of the $Sn_{1-x}Cu_{x/3}Sb_{2x/3}O_2$ form is obtained. We mention that $Cu_4SbO_{4.5}$ does not dissolve in the SnO_2 matrix, but probably by forming a eutectic melt it will improve the densification properties [12].

The purpose of the present paper was to study the correlation structure-microstructure-electrical characteristics and the anode polarisation of the SnO_2-based ceramics.

2. Experimental

The oxide mixtures were prepared from reagent grade (Merck) SnO_2, Sb_2O_3 and CuO. The powders with grain sizes below 60 µm were homogenized wet. Cylindrical samples with ⌀ = 10 mm and variable heights obtained by pressing at 30 MPa were heated to 1400 °C with a 4 hours plateau. A heating rate of 10 °C/min and cooling rate of 20 °C/min was used. After the thermal treatment the samples were analysed by X-ray diffraction, IR spectroscopy and electron microscopy. The ceramic properties density (d), porosity (P_a) and linear shrinkage ($\Delta l/l$) were determined. To ensure a good electrical contact during the run of experiments, the pellets were polished and gold plated by a special treatment [16].

The resistivity measurements were carried out with a B-641/Wyne Kerr autobalance bridge, in low impedance scheme, connected to an especially designed conductivity cell [16] over a temperature range from 20 to 1000 °C.

Seebeck effect measurements were performed with a special device built up in the NIPM laboratory [17].

The anodic polarization curves were obtained by current-voltage measurements under galvanostatic conditions. Speeds of 3 - 5 steps/min at 10 - 30 mA were applied at increasing and decreasing current [8].

Table 2. Microstructure and electrical characteristics of the studied samples.

Samples	Microstructures	$\chi_{970\,°C}$ (S·cm^{-1})	$\Delta E_{d,200-600°C}$ (eV)	C_s (μV/K)
S_1	pores	0.251	0.01	–12.3
S_2	liquid phase	0.538	–	–
S_3	pores	0.498	0.25	–25.8
S_4	$Cu_4SbO_{4.5}$ traces	0.590	0.3	–1.8
S_5	$Cu_4SbO_{4.5}$ traces	0.716	0.25	–1.7

3. Results and Discussions

3.1. Structural, Ceramic, and Electrical Characteristics

The studied samples were labelled with symbols from S_1 to S_5. Their initial compositions are listed in the Table 1.

According to the initial composition and CuO/Sb_2O_3 molar ratio (Table 1) the terms of the paragenesis of the samples have been considered belonging to the following systems:

S_1:	SnO_2-Sb_2O_3	binary system,
S_2:	SnO_2-CuO-Cu_2O	ternary system,
S_3:	SnO_2-$CuSb_2O_6$-Sb_2O_4	pseudoternary system.
S_4-S_5:	SnO_2-$CuSb_2O_6$-$Cu_4SbO_{4.5}$	

After thermal treatment, the X-ray diffraction data indicate the formation of a rutile type solid solution ($SnO_{2(ss)}$) as unique phase (Table 1).

A slight contraction of the elementary cell volume of the solid solution compared with SnO_2 was evidenced (Table 1).

The ceramic properties, namely apparent porosity (P_a), linear shrinkage ($\Delta l/l$) and density (d), also presented in Table 1, pointed out an inadequate sintering of the S_1 and S_3 samples.

In Table 2 the microstructure and the electrical characteristics (conductivity, activation energy, and

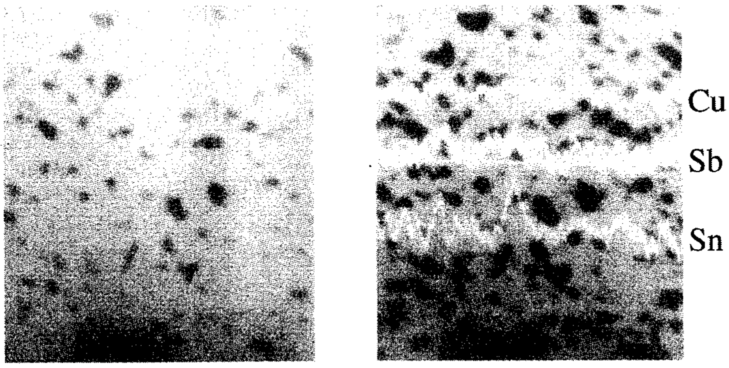

a) b)

Fig. 1. Microstructure of the S_3 sample. a) Image of the composition; b) profile of the composition.

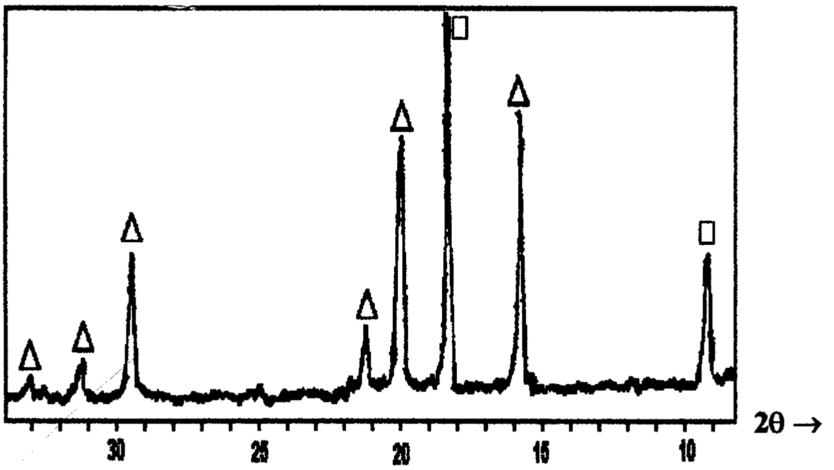

Fig. 2. X-Ray diffraction spectrum for the S_5 sample. ■: $Cu_4SbO_{4.5}$; Δ: $SnO_{2(SS)}$.

Seebeck coefficient) of the samples are presented. The presence of liquid phase (sample S_2), pores (samples S_1 and S_3) and $Cu_4SbO_{4.5}$ traces (samples S_4 and S_5) is mentioned in column 2 of Table 2.

It is well known that the presence of the liquid phase improves the sintering ability of CuO doped SnO_2 (the case of the sample S_2). The high porosity (Table 1) of the S_1, S_3 samples indicate the presence of the open pores. Figure 1 shows the porous surface of the S_3 sample.

Thermal treatment over 1200 °C makes $SnO_{2(ss)}$ unstable [18]. The following reactions take place:

$$S_1\colon SnO_{2ss} \xrightarrow{t^0>1200\,^\circ C} (1-x)SnO_{2ss} + xSnO_2 + ySb_2O_3 \uparrow$$

$$S_3\colon SnO_{2ss} \xrightarrow{t^0>1200\,^\circ C} (1-x)SnO_{2ss} + xSnO_2 + yCuSb_2O_6 + zSb_2O_3 \uparrow$$

and can increase the pore volume.

The samples S_4 and S_5 belong to the SnO_2-$CuSbO_6$-$Cu_4SbO_{4.5}$ pseudoternary system containing beside $SnO_{2(ss)}$ very small amounts of $Cu_4SbO_{4.5}$ which does not dissolve in the SnO_2 matrix.

The X-ray diffraction spectrum at the surface of the sample S_5, presented in Fig. 2, confirms the presence of this compound, preferentially oriented.

The electrical conductivity $\chi = 1/\rho$ at 970 °C, calculated from experimental resistivity data ($\rho = R\frac{S}{l}$, where R and S stand for the resistance and area of the sample section, respectively, and l is the distance of the voltage contact), is listed in Table 2. The electrical conductivity is quite high in all samples at this temperature, and in agreement with the microstructure of the samples. The highest value of the conductivity was found for the sample S_5 according to its high density and large charge carrier number.

The activation energy (ΔE_d), determined from the linear dependency of the $\ln\chi$ vs. $1/T$ with an Arrhenius type relation

$$\chi = \chi_0 e^{\Delta E_d/RT},$$

is also given in Table 2. The values range from 0.01 to

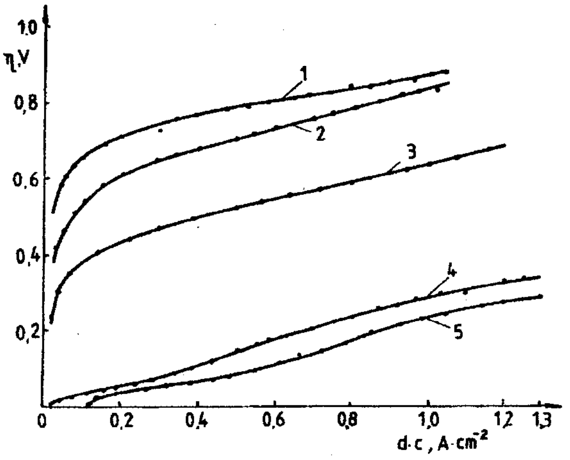

Fig. 3. The evolution of anodic overvoltage vs. current density on different anodes. 1: vitrous carbon; 2: graphite; 3: pretreated carbon; 4: SnO_2-based inert; 5: Pt.

0.3 eV, suggesting electronic type conduction for all investigated samples. The values of the Seebeck coefficient (Table 2) obtained in this investigation support this viewpoint.

3.2. Electrochemical Behaviour in the Cryolite-alumina Melts

It is well known that the Hall-Heroult process for aluminium production uses consumable carbon anodes. The cell reaction is the following:

$$^{1}/_{2}\, Al_2O_3 + {}^{3}/_{4}\, C = Al + {}^{3}/_{4}\, CO_2,\ E_{rev} = 1.169\ \mathrm{V}.$$

The anode product, when inert anodes are used, is oxygen, and the cell reaction is

$$^{1}/_{2}\, Al_2O_3 = Al + {}^{3}/_{4}\, O_2,\ E_{rev} = 2.196\ \mathrm{V}.$$

This large difference in emf between those 2 processes is partly offset by higher overvoltage on carbon (0.4 - 0.6 V) than on SnO_2-based inert anodes, see Figure 3.

The overvoltage increases with the current density at 970 °C and an obvious difference between the overvoltage of carbon, Pt and SnO_2-based anodes is noted. The anodic process of SnO_2-based anodes occurs with 3 - 4 times lower overvoltage than of carbon anodes, and similar to Pt inert anodes.

In Fig. 4 we present anodic polarization curves of the studied samples, comparatively with those of Pt anodes, obtained in an electrolyte of composition 83wt% Na_3AlF_6 + 7wt% AlF_3 + 5wt% CaF_2 at 970 °C.

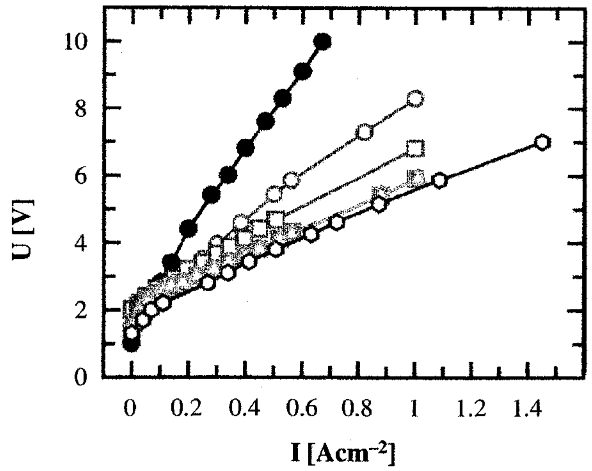

Fig. 4. Anodic polarization curves, obtained in an electrolyte of composition 83% Na_3AlF_6 + 7% Al_2O_3 + 5% CaF_2 at 970 °C. ○ (gray): SnO_2 + 2%Sb_2O_3; ●: SnO_2 + 2%CuO; □: SnO_2 + 2%Sb_2O_3 + 0.5%CuO; ■: Pt; Δ: SnO_2 + 1%Sb_2O_3 + 1%CuO; ○: (dark) SnO_2 + 2%Sb_2O_3 + 2%CuO.

At the current density of 0.8 Acm^{-2} (which is used in industry) the highest voltage was found on the S_2 sample. This sample contains a small amount of SnO_2-CuO-CuO_2 ternary eutectic melts, which can act as a potential barrier.

The samples S_1 and S_3, that present the higher apparent porosity (open pores), also exhibit a high voltage.

Voltages similar to those on Pt were obtained on the samples S_4 and S_5. It was noticed that the lowest potential was obtained for the sample S_5, which also has the highest electrical conductivity and the porosity zero.

The presence of the microphase $Cu_4SbO_{4.5}$ at the working temperature (970°C) did not distort the electrical behaviour. Indeed Shimada and Mackenzie [19] identified in the 380 - 1000 °C temperature range, in air, the following chemical reaction:

$$Cu_4SbO_{4,5} \xleftrightarrow{380\,-\,1000\,^{\circ}\mathrm{C,\ in\ air}} CuSb_2O_6,$$

which could improve an additional incorporation of $CuSb_2O_6$ in the SnO_2 labilized lattice.

The ohmic drops (measured by the interruption current method and with an oscilloscope) on all those electrodes were very high, varying in the range 2.2 to 7 V at 0.8 Acm^{-2}.Those high ohmic drops exist because of the high resistance in the electrolysis circuit.

4. Conclusion

This study makes for the first time an exhaustive investigation of the structure and electrochemical behaviour of SnO_2-based inert anodes.

All the studied samples were presented as a rutile type solid solution, but with different microstructure. The electrical conductivity and the anodic polarization were closely associated with the microstructure of the samples.

[1] W. Zimba, B. Zimba, and I. Szklo, Ceram. **24**, 12 (1973).

[2] H. Alder, U.S. Patent, 40 57 480 (1977).

[3] R. D. Secrist, M. F. Clark, U.S. Patent, 44 84 977 (1984).

[4] E. A. Varella, D. Gonevea, E. Longo, N. Dolet, M. Orillon, and E. P. Bonnet, Diffus. Defect Data, Pt.B, 25 (1992).

[5] M. Zaharescu, S. Mihaiu, S. Zuca, and K. Matiasovsky, J. Mater. Sci. **26**, 1666 (1991).

[6] S. Zuca, M. Terzi, M. Zaharescu, and K. Matiasovsky, J. Mater. Sci. **26**, 1673 (1991).

[7] S. Zuca, A.-M. Popescu, N. Ene, V. Constantin, Revista de Chimie **50**, 42 (1999).

[8] A.-M. Popescu, Ph.D-Thesis, Bucharest 1998.

[9] A.-M. Popescu and V. Constantin, Rev. Roum. Chim. **43**, 793 (1998).

[10] A.-M.Popescu, S. Zuca, S. Mihaiu, and V. Constantin, Progress in Molten Salt chemistry 1, Protf. N. J. Bjerrum Special Volume, ed. R. W. Berg and H. A. Hjuler, Elsevier, Amsterdam 2000, p. 417.

[11] A.-M. Popescu, S. Mihaiu, Proc. ICETS-Session 3 / Advanced Materials, ed. J. Song and R. Yin, New World Press, Vol. 2, 1156 (2000).

[12] M. Zaharescu, S. Mihaiu, D. Crisan, and S. Zuca, 3rd Euro Ceramics, ed. P. Duran and F. F. Fernandez, faenza, editura Iberica **2**, 359 (1993).

[13] M. Stan, S. Mihaiu, D. Crisan, and M. Zaharescu, Eur.& Solid Inorg. Chem. **35**, 254 (1998).

[14] S. Mihaiu, O. Scarlat, C. Radovici, and M. Zaharescu, Proc. 6th ECERS, Brighton, U.K. **2**, 68 (1999).

[15] S. Shimada and T. Ishii, Reactivity of Solids **7**, 183 (1989).

[16] S. Zuca, S. Mihaiu, and M. Zaharescu, 4th ECERS, Electroceramics, ed. G. Gusmano and E. Traverse, Italy, Vol. 5, 373 (1995).

[17] E. Jaklovszky, R. Ionescu, and N. Nistor, Electrochimica **22**, 105 (1974).

[18] S. Mihaiu, O. Scarlat, C. Radovici, and M. Zaharescu, Proc. 13th Conf. Glass & Ceramics, Varna, Bulgaria, ed. B. Sarmoneva, S. Bacharova, I. Gutzov, and I. Dimitrov, Sofia, Vol. 2, 75 (1999).

[19] S. Shimada and K. D. Mackenzie, Termochim. Acta **56**, 73 (1982).